Journal of Materials and Environmental Sciences
ISSN : 2028-2508
CODEN : JMESCN

J. Mater. Environ. Sci., 2018, Volume 9, Issue 9, Page 2615-2623

http://www.jmaterenvironsci.com

New thermodynamic assessment of the Ruthenium-Tin system

M. Idbenali[1,2*], C. Servant[3]

[1.] *Centre régional des métiers de l'enseignement et de la formation, Souss Massa Morocco*
[2.] *Laboratoire de Mécanique, Procédés de l'Energie et de L'Environnement (LMP2E), ENSA, Agadir , Morocco*
[3.] *Laboratoire de Physicochimie de l'Etat Solide, ICMMO, Université de Paris-Sud, 91405 Orsay Cedex France*

Received 12 Aug 2017,
Revised 11 Apr 2018,
Accepted 26 Apr 2018

Keywords

- ✓ Phase diagram;
- ✓ Thermodynamic;
- ✓ Assessment;
- ✓ CALPHAD;
- ✓ Ru-Sn

M. Idbenali
idbenalimohamed@yahoo.fr
0610452332

Abstract

The Ru-Sn system has been assessed by means of the Calphad approach. The liquid phase has been described with the association solution model with 'Ru_3Sn_7' as an associated complex. The solution phases ((Ru) and (Sn)) were modeled with the sublattice formalism and the excess term of the Gibbs energy with the Redlich-Kister equation. The Ru_2Sn_3 and Ru_3Sn_7 phases have been treated as stoichiometric compounds. The calculated phase diagram and the thermodynamic properties of the system are in satisfactory agreement with the experimental data.

1. Introduction

The early investigations on the Ruthenium-Tin system were carried out by Shwomma et al [1] who drew a diagram containing three intermediate phases: Ru_2Sn_3, Ru_2Sn and Ru_3Sn_7. Ru_2Sn_3 formed by the peritectoid reaction Ru2Sn3 <-> (Ru) +$RuSn_2$ at T=1373±10K, Ru_3Sn_7 is a congruently melting compound (Temperature not determined), $RuSn_2$ formed by the peritectic reaction Ru_2Sn<-> liq+Ru_3Sn_7 (T unknown), decomposed by eutectoid transformation $RuSn_2$ <-> Ru_2Sn_3 +Ru_3Sn_7 at T=973K. The same authors have reported the crystal structures of all the intermetallic compounds. Later, Susz [2] confirmed the occurrence of only two intermetallic compounds: Ru_3Sn_7, melting congruently at T=1548±2K, and Ru_2Sn_3 with a peritectoid decomposition Ru_2Sn_3<-> (Ru) + Ru_3Sn_7 at T=1513±5 K. Susz [2] found two eutectics: Liquid <-> (Sn) + Ru_3Sn_7 at T=493K and Liquid <-> Ru_3Sn_7 + (Ru) at 1531±5K. The maximum solubility of Sn in Ru at T = 1639K, $x_{Sn} = 0.02$.

Massalski et al. [3] preferred the diagram proposed by Shwomma et al [1]. In 1996, Perring et al. [4] have completely revised the Ru-Sn phase diagram by differential thermal analysis (DTA), X-ray diffraction, and microprobe measurements. The authors confirm the existence of the two phases Ru_2Sn_3 and Ru_3Sn_7: Ru_2Sn_3 decomposed by peritectic reaction at T = 1539±4 K and Ru_3Sn_7 has a congruent melting at T=1530±2K. Kawabata et al. [5] examined the liquidus boundaries by thermal analysis, segregation method and solid state emf measurements (using calcia stabilized zirconia solid electrolyte).

Charles et al. [6] attempted to assess the phase diagram using the software NancyUn elaborated by Charles et al. [7]. This routine is less powerful than the Thermocalc software [8] because it took into account only the liquid and the terminal solid solutions (Ru) and (Sn) were not modeled. Using the spot technique, Ananthasivan et al. [9] measured the liquidus of Ru-Sn system in the composition range from 35 to 100 at.% Sn. Both Ru_2Sn_3 and Ru_3Sn_7 were reported to decompose peritectically, i.e. liquid + Ru<-> Ru_2Sn_3, liquid + Ru_2Sn_3<-> Ru_3Sn_7. A monotectic invariant reaction, i.e. liquid 1 <-> Ru + liquid 2, was detected at 1297±7 K and 37 at.%Sn. Recently, Long et al. [10] established a thermodynamic optimization of the Ru-Sn binary system with the Thermo-Calc software [8], In the assessment by [10]

Ru_3Sn_7 is stable at very high temperatures when the liquid phase is suspended and the calculated integrals and enthalpies and entropies of liquid phase are different with the measured ones by Kawabata et al [5]. In addition, the crystal structures of the various phases are reported in Table 1.

As our contribution to this field, it was therefore necessary to completely re-assess the thermodynamic parameters for the Ru-Sn system taking into account most of the experimental data, and by imposing additional constraints to avoid the appearance of an unwanted inverted miscibility gap in the liquid phase during the phase diagram calculation up to 6000 K.

Table1. Symbols and crystal structures of the stable solid phases in the (Ru_Sn) alloys

Symbols des phases	Composition at %Sn	Symbol used in Thermo-Calc data file	Space group	Prototype
(Ru)	0	Hcp_A3	P63/mmc	Mg
Ru_2Sn_3	60	Ru_2Sn_3	$I4_1/amd$	Ru_2Si_3
Ru_3Sn_7	70	Ru_3Sn_7	Im3m	Ru_3Sn_7
(Sn)	100	Bct_A5	$I4_1/amd$	Sn

(Ru) : Ruthenium
(Sn) : Tin

2. Review of the literature data

Several thermodynamic information is available in the literature concerning the Ru-Sn system [4-6, 11-13]. The enthalpies of formation of Ru_2Sn_3 and Ru_3Sn_7 at 1173K have been measured by Perring et al.[4] using direct reaction calorimetry. Later, Ciccioli et al.[11] obtained the enthalpy data at 298 K, by measuring vapor pressure, which was in agreement with the data from Perring et al.[4]. Kuntz et al.[12] determined the molar heat capacities of Ru_2Sn_3 and Ru_3Sn_7 by differential scanning calorimetry in the temperature range 310 to 1076K.

Kawabata et al.[5] explored the liquid Ru-Sn at high temperature (1300 to 1800 K, x(Sn)> 0.6) in order to determine Tin activity by the electromotive force (emf) method. In addition, Meschel and Kleppa [13] have been measured the standard enthalpy of formation of Ru_3Sn_7 by high temperature calorimetry. In 1999, Charles et al. [6] measured the enthalpy of formation of Ru_2Sn_3 and Ru_3Sn_7 intermetallic compounds by direct calorimetry. All information cited in above was used in our optimization.

3. Thermodynamic models

3.1. Pure elements

The Gibbs energy function $G_i^{\phi}(T) = {}^0G_i^{\phi} - H_i^{SER}$(298.15K) for the element i (i=Ru,Sn) in the Φ phase (Φ = Liquid, BCT and HCP is described by an equation of the following form:

$$G_i^{\phi}(T) = a + bT + cTlnT + dT^2 + eT^3 + fT^7 + gT^{-1} + hT^{-9} \quad (1)$$

where: H_i^{SER} (298.15K) is the molar enthalpy of the element i at 298.15K in its standard element reference (SER) state, BCT for Tin and HCP for Ruthenium. In this paper, the Gibbs energy functions are taken from the SGTE compilation of Dinsdale [14].

3.2. Liquid phase

The liquid phase has been described by the association model by Sommer [15]. The association model is based on the hypothesis that a C complex is formed in the liquid phase (where A and B are pure elements initially present in the mixing) as follows:

$$pA + qB <=> ApBq \quad (1bis)$$

(ApBq) corresponds to the C complex with p and q the stoichiometric coefficients). Such a formation of a C complex in the liquid phase can be suggested by the experimental enthalpies of formation of the intermetallic phases which show a nearly triangular shaped concentration dependence. As in the Ba-Pb [16], Yb-Pb [17] and Ca-Pb [18] systems, the compound which presents the highest melting point and enthalpy of

formation has been taken as the associated complex. Ru3Sn7 is the most probable liquid associated complex (C). Therefore, the Gibbs energy of one mole of formula unit is expressed as the sum of four terms:

$$G^{liq} - H^{SER} = {}^{ref}G^{liq} + {}^{form}G_C^{liq} + {}^{id}G^{liq} + {}^{ex}G^{liq} \qquad (2)$$

With

$${}^{\text{ref}}G^{\text{liq}} = \left[x_{Sn}({}^{0}G_{\text{Sn}}^{\text{liq}} - H_{\text{Sn}}^{\text{SER}}) + x_{\text{Ru}}({}^{0}G_{\text{Ru}}^{\text{liq}} - H_{\text{Ru}}^{\text{SER}})\right](y_{\text{Ru}} + (p+q)yc + y_{Sn}) \qquad (3)$$

$${}^{\text{f}}G_C^{\text{liq}} = \left[y_{Sn}\ G_{\text{Sn}}^{\text{liq}}(T) + y_{\text{Ru}}(\ G_{\text{Ru}}^{\text{liq}}(T) + y_{\text{C}}({}^{0}G_{\text{C}}^{\text{liq}}(T)\right] \qquad (4)$$

$${}^{\text{id}}G_C^{\text{liq}} = RT(y_{Sn}Ln(y_{Sn}) + y_{Ru}Ln(y_{Ru}) + y_C Ln(y_C)) \qquad (5)$$

${}^{0}G_{\text{C}}^{\text{liq}}(T)$ Gibbs energy function for the associated species, R is the perfect gas constant and T is the temperature

The A, B, C three species in the liquid phase have y_A, y_B and y_C as mole fraction normalised to $y_A + y_B + y_C = 1$. x_{A} and x_B are the absolute mole fractions of the two components A and B of the liquid, without considering the associated species, normalized to $x_B + x_{\text{A}} = 1$.

For a regular liquid solution $C_{Ru,Sn}^{reg}$, in [15] is equal to the ${}^{0}L_{Ru,Sn}^{Liq}$ term of the Redlich–Kister polynomial [19] of the ${}^{ex}G^{liq}$ energy part in Eq. (2):

$${}^{ex}G_{liq} = y_i\ y_j \sum_{\nu=0}^{\nu} {}^{\nu}L^{liq}{}_{i,j}(y_i - y_j)^{\nu} \qquad (6)$$

In this work ν =0 (Table 2).

$${}^{ex}G_{liq} = y_{Ru,}y_{Sn}\ {}^{à}L^{liq}{}_{RuSn} + y_{Ru,}y_{Ru3Sn7}\ {}^{à}L^{liq}{}_{RuRu3Sn7} + y_{Sn}y_{Ru3Sn7}\ {}^{à}L^{liq}{}_{Sn,Ru3Sn7}$$

with *i* and *j* are indices which correspond to the three species Ru, Sn and Ru3Sn7.
In this work ν =0 (Table 2).

The binary interaction parameters of the ${}^{0}L_{i,j}^{Liq}$ type, evaluated in the present work, were temperature dependent as follows: ${}^{0}L_{i,j}^{Liq} = a_0 + b_0 T$ (7)
a_i and b_{i} are the coefficients to be optimized.

3.3. Solution phases

The Gibbs energy of one mole of formula unit is expressed as the sum of three terms:

$$G^{\Phi} - H^{\text{SER}} = {}^{\text{ref}}G^{\Phi} + {}^{\text{id}}G^{\Phi} + {}^{\text{ex}}G^{\Phi} \qquad (8)$$

$${}^{\text{ref}}G^{\Phi} = x_{\text{Ru}}\left[{}^{0}G_{\text{Ru}}^{\Phi} - H_{\text{Ru}}^{\text{SER}}\right] + x_{\text{Sn}}\left[{}^{0}G_{\text{Sn}}^{\Phi} - H_{\text{Sn}}^{\text{SER}}\right] \qquad (9)$$

where $H_{\text{i}}^{\text{SER}}$ (298.15 K) is the molar enthalpy of the *i* element at 298.15 K in its Standard Element Reference (SER) state, BCT for Tin and HCP for Ruthenium.

$${}^{\text{id}}G^{\Phi} = RT(x_{\text{Ru}} \ln x_{\text{Ru}} + x_{\text{Sn}} \ln x_{\text{Sn}}) \qquad (10)$$

Where R is the ideal gas constant; T is the temperature, in Kelvin; x_{Ru} and x_{Sn} are the mole fraction of the elements Ruthenium and Tin, respectively.

The ${}^{\text{ex}}G\Phi$ energy part in Eq. (2) is given by the Redlich–Kister polynomial [19]

$$^{ex}G^{\Phi} = y_i\, y_j \sum_{\lambda=0}^{\lambda} {}^{\lambda}L_{i,j}^{\Phi}\,(y_i - y_j)^{\lambda} \qquad (11)$$

y_i and y_j denotes the site fraction in the sublattice, i and j the indices which correspond to the two species Rutheniumum and Tin and $y_i + y_j = 1$

The binary interaction parameters of the $^{\lambda}L_{i,j}^{Liq}$ type, assessed in the present work, were temperature dependent, as follows:

$$^{\lambda}L_{i,j}^{\Phi} = a_{\lambda} + b_{\lambda}T \qquad (12)$$

with the excess entropy $s = -\ b_{\lambda}$ (knowing for example that for lambda=0, excess entropy versus composition is calculated through this coefficient – *b* and is then $y_i * y_j * b$).

a_{λ} and b_{λ} are the coefficients to be optimized.

3.4. Stoichiometric compounds

The Ru_2Sn_3 and Ru_3Sn_7 were considered as stoichiometric compounds. Its Gibbs energy noted as $^{0}G_{ApBq}$ was expressed as follows: $^{0}G_{ApBq} = a + bT + cTLn(T) + dT^2$ (13)

Where *a ,b, c* and d are parameters to be determined.

Table 2 . The optimized thermodynamic parameters for solid solution phases of the Ru-Sn system

Phase	Thermodynamic model	Parameters / J mol $^{-1}$
Liquid (Ru ,Sn, Ru3Sn7)	(Ru ,Sn, Ru3Sn7)	ΔH^{f}_{Ru3Sn7}=-413807.3692 ΔS^{f}_{Ru3Sn7} =22.8489709 $^{0}L_{Ru,Sn}$ = -48479.98899 +29.38512188.T $^{0}L_{Ru3Sn7,Sn}$ =10917.22482 -6.460795529.T
HCP_A3	$(Ru,Sn)_1\ (Va)_{0.5}$	$^{0}L^{HCP}_{Ru,Sn}$ = 50000
BCT_A5	(Sn)	No excess term
Ru_2Sn_3	$(Ru)_{0.4} : (Sn)_{0.6}$	ΔG^{f}_{Ru2Sn3}=-30223.63277+114.8005674.T-22.80554509.TLn(T)-0.0131882823.T^2
Ru_3Sn_7	$(Ru)_{0.3} : (Sn)_{0.7}$	ΔG^{f}_{Ru3Sn7}=-34973.07597+121.5120746.T-23.76169344.TLn(T)-0.0151980545.T^2

* (Va) for vacancy

4. Results and Discussion

The optimization of the model parameters was conducted using the PARROT module [20] in the Thermo-calc software package developed by Sundman et al. [8]. This module works by minimizing the square sum of the differences between experimental data and calculated values. In the optimization procedure, each set of experimental data was given a certain weight. The weights were changed systematically during the optimization until most of the experimental data were accounted for within the claimed uncertainty limits. The optimization was carried out by steps.

The parameters for the liquid phase were optimized first using the experimental (Gibbs energy enthalpy and entropy of the liquid phase) measured by Kawabata et al. [5]. The intermetallic compound Ru3Sn7 was added in data base of software by assessed the parameter a in equation 12 using enthalpy of formation of Ru3Sn7, measured Charles et al [6]. The parameter b was calculated by the congruent in phase diagram determined by Perring et al [4]. The parameters c and d were evaluated using molar heat capacity of Ru3Sn7 measured by Kuntz et al [12]. Afterwards, the compound Ru_2Sn_3 was optimized using the same process. The other parameters for the terminal solid solution phases were consequently optimized by using available phase diagram data.

All the parameters were finally evaluated together to give the best description of the system. All the optimized thermodynamic parameters are listed in Table 2. With these parameters, the phase diagram of Ru–Sn system is shown in Figs. 1a-1b and compared with the experimental data [4] in Fig. 2. We note a reasonable agreement between the calculated compositions and temperatures of the relevant invariant reactions and the experimental phase boundaries from [4].

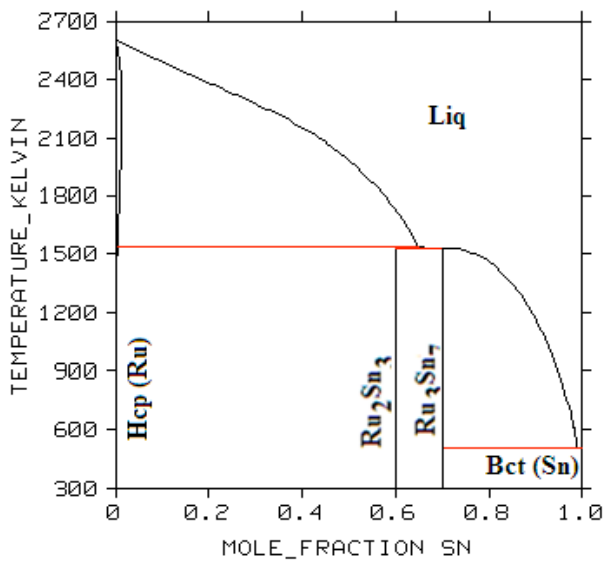

Figure 1a : Calculated phase diagram of Ru-Sn system

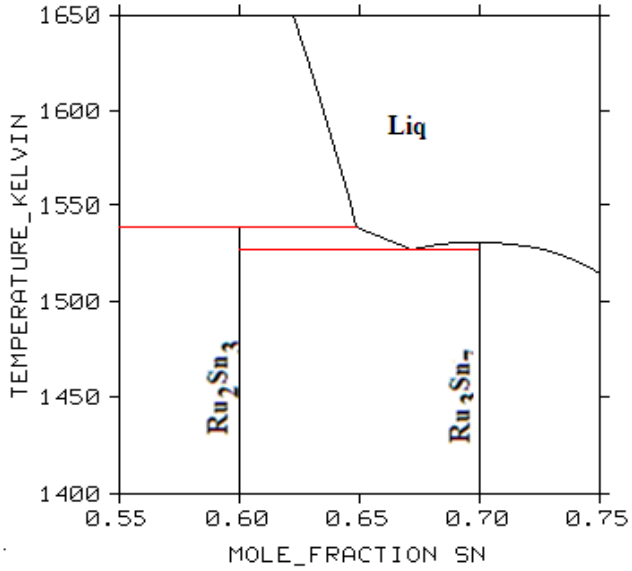

Figure 1b: Enlarged part on the Sn-rich side of the Ru–Sn phase diagram .

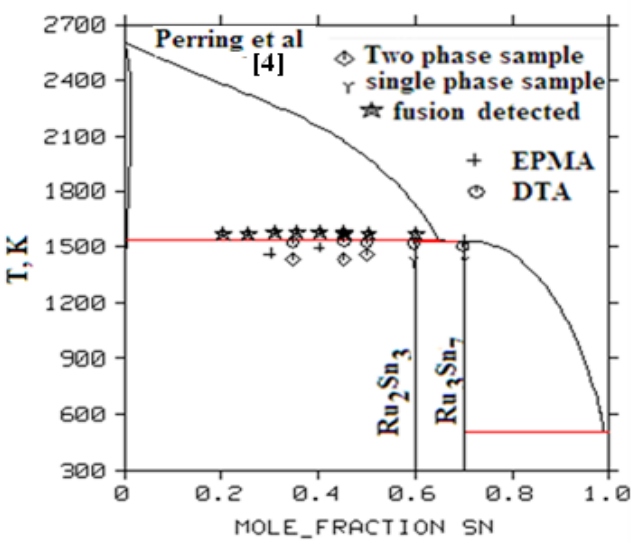

Figure 2: Calculated phase diagram of Ru-Sn system compared with the experimental values in [4]

The calculated compositions and temperatures of the invariant reactions in this binary system are summarized and confronted to the available experimental data in Table 3. Fig. 3 presents the calculated integral mixing Gibbs energy of the liquid at T=1573K compared with experimental values in [5].

Table 3. Invariant reactions in the Ru-Sn System

Invariant reactions	Susz et al [2]		Perring et al [4]		This work	
	T/ °C	X_{Liq},/ at% Sn	T / °C	X_{Liq}, / at% Sn	T / °C	X_{Liq}, / at%Sn
(Sn)bct + Ru_3Sn_7⇔Liq	493±20	99	506±3	99	504	98.96
Ru_3Sn_7⇔Liq	1548±5	70	1530±4	70	1530	70
Ru_2Sn_3⇔Liq+Hcp	1513±5	65	1539±4	65	1539	64.87
Ru_3Sn_7 + Ru_2Sn_3⇔ Liq	1531±5	67	1528±5	67	1527	67.19

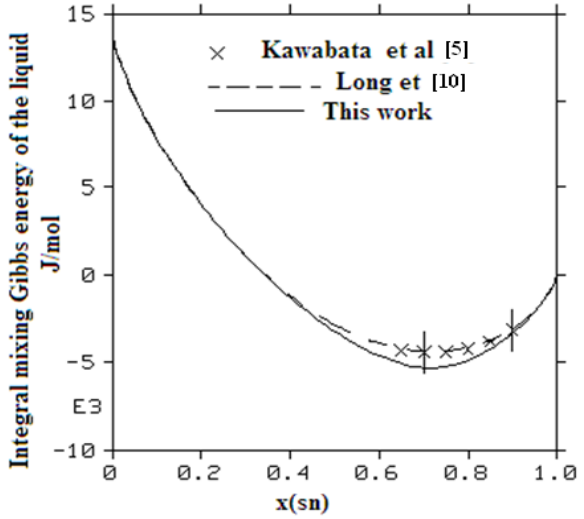

Figure 3. Calculated integral mixing Gibbs energy of the liquid at T=1573K compared to experimental values in [5]

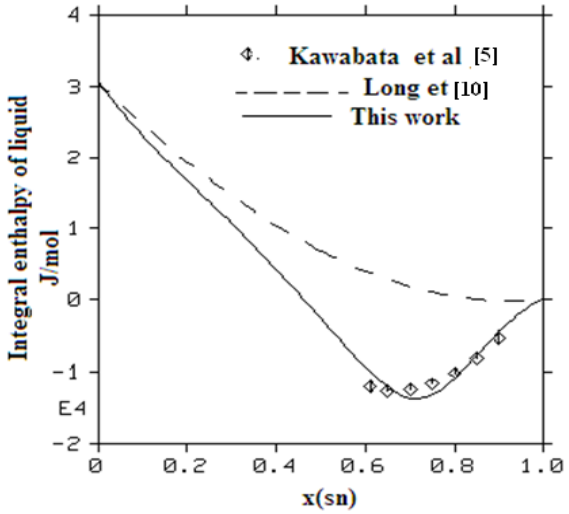

Figure 4: Integral mixing enthalpy of the liquid at T=1573K

The assessed enthalpy and entropy of mixing of the liquid at 1573K is plotted in Figs. 4-5 and it is clear that the calculated results are in good agreement with experimental data reported by [5]. The calculated chemical potential of elements Ruthenium and Tin with experimental data is illustrated in Fig. 6 show that the fit to the experimental data is excellent. In Figs. 7a and b the calculated activities of Sn and Ru at 1573K seem to be so perfectly identical with experimental date from [5].

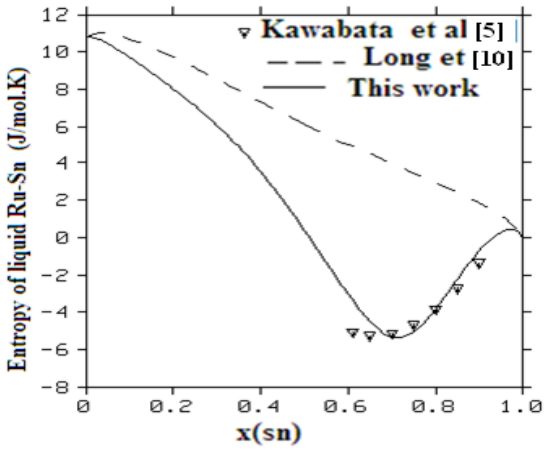

Figure 5: Integral entropy of the liquid at T=1573K

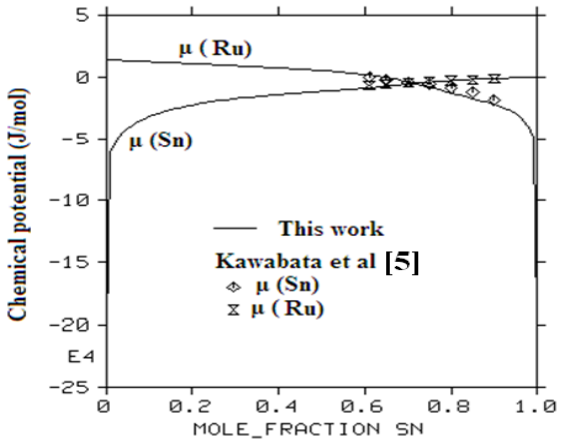

Figure 6 : Chemical potential of Ru and Sn compared with experimental values in [5] at T=1573K

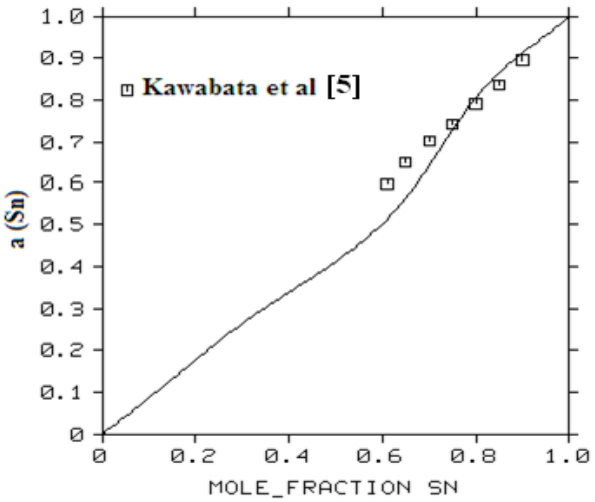

Figure 7a: Calculated activities of Sn at 1573 in the Ru-Sn system compared with the experimental data [5]

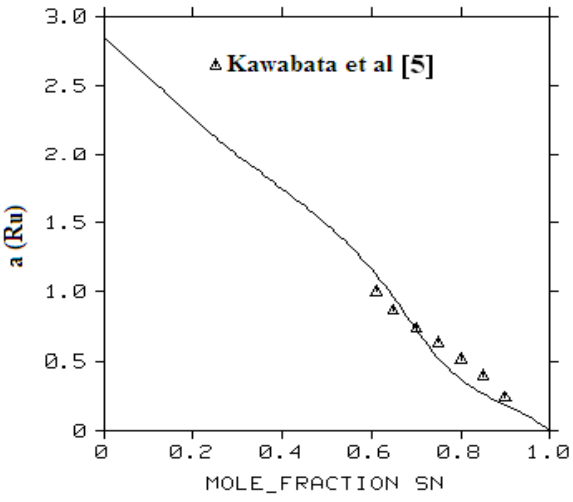

Figure 7b : Calculated activities of Ru at 1573 in the Ru-Sn system compared with the experimental data [5]

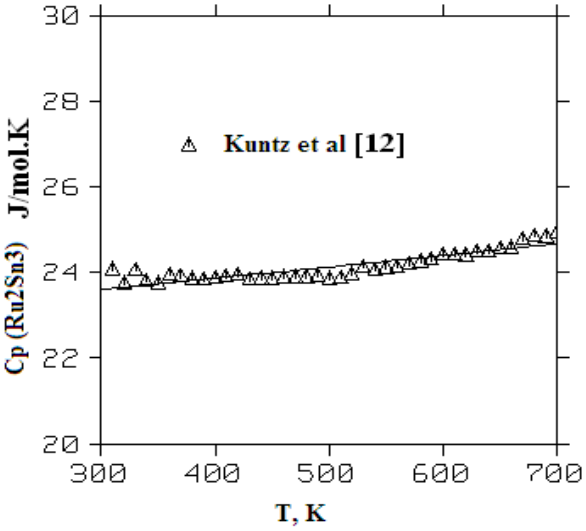

Figure 8a: Calculated and measured molar heat capacity of Ru_2Sn_3 (J/mol.K)

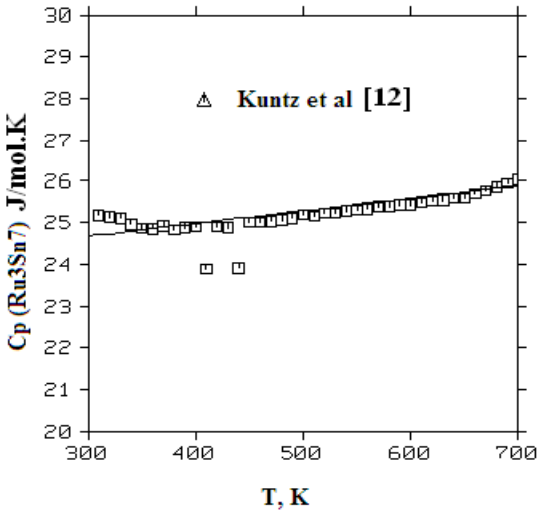

Figure 8b: Calculated and measured molar heat capacity of Ru_3Sn_7 (J/mol.K)

All thermodynamic data cited are listed in Table 4. As shown in Figs. 8a-b, the calculated molar heat capacity of Ru_2Sn_3 and Ru_3Sn_7 compared with the experimental data in [12] (see Table 5.) .

Table 4. Thermodynamic Properties of the System Ru , Sn at 1573 K

x(Sn)	G^M_{Liq} (J/mol)	H^M_{Liq} (J/mol)	S^M_{Liq} (J/mol.K)	μ(Ru) (J/mol)	μ(Sn) (J/mol)	a(Ru)	a(Sn)	Ref
0.90	-3200	-5320	-1.35	-19000	-1450	0.236	0.895	[5]
	-2956	-4400	-0.9179	-18573	1172	0.2259	0.9177	This work
0.85	-3840	-8070	-2.69	-12400	-2340	0.389	0.836	[5]
	-3737	-7862	-2.623	-13995	520.4	0.3227	0.8724	This work
0.80	-4230	-10200	-3.81	-8900	-3070	0.508	0.791	[5]
	-4259	-11134	-4.37	-9689	-395.3	0.4466	0.8142	This work
0.75	-4410	-11700	-4.65	-6000	-3890	0.632	0.743	[5]
	-4514	-13414	-5.658	-5098	-1733	0.6226	0.7392	This work
0.70	-4450	-12500	-5.13	-4100	-4610	0.733	0.703	[5]
	-4481	-13720	-5.873	-554.3	-3454	0.8551	0.6555	This work
0.65	-4300	-12600	-5.24	-2000	-5630	0.864	0.650	[5]
	4181	-11926	-4.923	2984	-5148	1.098	0.5815	This work

As described in Fig. 9 and in table 5, the standard enthalpies of formation assessed in this work show the general tendency similar to experimental data [6]. As mentioned in [21], in order to check that the optimized thermodynamic parameters of the intermetallic compounds are satisfactory, we verified that when the liquid phase is suspended during the calculation of the Ru–Sn phase diagram, the stoichiometric phases disappear at high temperatures, the terminal solid solutions and a two-phase domain existing between them are calculated, Fig. 10. It will be noted that only the (Ru–Sn) HCP_A3 solid solution is calculated on the whole Sn composition range and not the BCT_A5 (Sn) one in the Sn-rich region. This is due to the power series in terms of temperature for the Sn element in the HCP_A3 state which becomes metastable compared with the BCT_A5 state at higher temperatures [14].

Table 5. Thermodynamic Properties of intermetallic compounds

	Ru_2Sn_3			Ru_3Sn_7		
T(K)	Cp J/mol.K		ΔH^f kJ/mol	Cp J/mol.K		ΔH^f kJ/mol
	[12]	This work	-24.3±1.6 [6]	[12]	This work	-25.4±0.8 [6]
310	24.04	24.05		25.17	24.74	
330	24.03	24.05	-21.6±3 [4]	25.10	24.81	-23.7±1.6 [4]
350	23.71	23.76	-21.1±2.5 [11]	24.86	24.78	-20.8±2.9 [11]
370	23.87	23.80	-	24.91	24.81	-18.7 [13]
390	23.80	23.84	-23.31 This work	24.87	24.96	-27.75 This work
410	23.87	23.91		24.89	25.03	
430	23.80	23.98		24.87	25.10	
450	23.83	24.02		25.00	25.14	
480	23.86	24.05		25.05	25.25	
520	23.94	24.16		25.22	25.39	
540	24.03	24.27		25.27	25.43	
580	24.22	24.34		25.38	25.54	
600	24.38	24.45		25.42	25.61	
630	24.45	24.49		25.52	25.72	
660	24.54	24.56		25.69	25.83	
690	24.80	24.80		25.94	25.90	

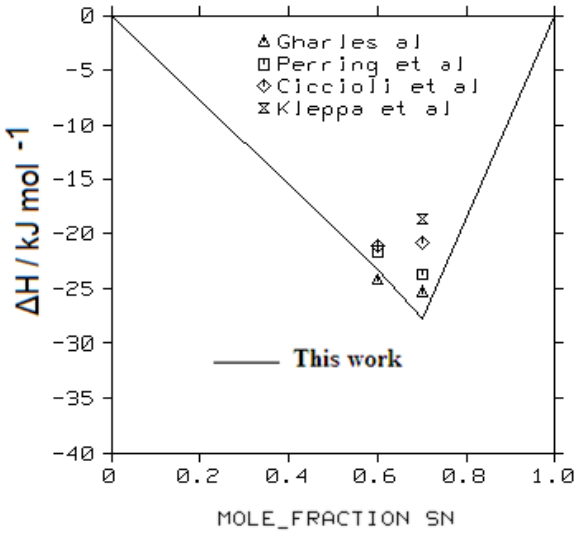

Figure 9: Calculated and measured enthalpies of formation of the intermetallic compounds.

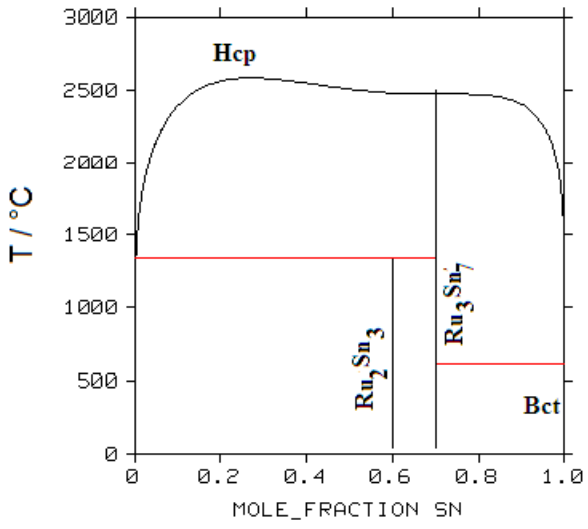

Figure 10: Calculated Ru–Sn phase diagram when the liquid phase is suspended

Conclusions

The Ru–Sn binary system has been reoptimized by using all experimental data from phase diagram and thermodynamic properties. A consistent set of thermodynamic parameters was derived. Compared to the previous assessment by Long et al. [10], the present reassessment used:

- ✓ Chemical potential of elements Ruthenium and Tin measured by Kawabata et al [5] not mentioned in the work in [10].
- ✓ The activities of Sn and Ru at 1300°C determined by [5].
- ✓ The entropy of liquid phase measured by Kawabata et al [5].
- ✓ The compounds are stable up to high temperatures and the intermetallic phase Ru3Sn7 not is stable at very high temperatures when the liquid phase is suspended see figure 10.
- ✓ A better agreement with the experiments by Kawabata et al. [5] than the one obtained by Long et al. [10] of the integral enthalpies and entropies of mixing of the liquid phase calculated at T=1573K.

Finally, we verified that no miscibility gap was calculated with our thermodynamic optimized parameters for the liquid phase. The computed values are in good agreement with the phase diagram data and experimental thermodynamic data.

References

1. O. Schwomma, H. Nowotny, and A. Wittman, *Monatsh,. Chem*., 95 (1964) 1538-1542.
2. C.P. Susz, thesis , Université de Genève, France, 1976.
3. Massalski TB (ed.) Binary alloy phase diagrams, 2nd ed. Materials Park: ASM International, (1990).
4. L. Perring, P. Feschotte, F. Bussy and J.C. Gachon. *J. Alloy.Compd*., 245 (1996) 157-163.
5. R. Kawabata, M. Myo-Chin, and M. Iwase. *Metall. Mater. Trans B*, 29 (1998) 577-581
6. J. Charles, L. Perring, J.J. Kuntz and J.C. Gachon. *J. Phase Equilib*., (1999); 20: 573-580.
7. J. Charles, J.C. Gachon, and J. Hertz.. *Calphad,* 9 (1985) 35-42.
8. B.Sundman , B. Janson, J-O. Andersson. *Calphad.* 9 (1985) 153–190.
9. K. Ananthasivan, I. Kaliappan, and P.R. Vasudeva Rao. *J. Nucl. Mater*.,305 (2002) 97-105.
10. Zhaohui Long, Fucheng Yin, Yajun Liu, Jiang Wang, Huashan Liu, Zhanpeng Jin., *J. Phase Equilib*. 33 (2012) 97–105.
11. A. Ciccioli, G. Balduci, G. Gigli, L. Perring, J.J. Kuntz, and J.C.Gachon, Ber. Bunsenges.. *Phys. Chem.* 102 (1998) 1275-1278.
12. J.J. Kuntz, L. Perring, P. Feschotte, and J.C. Gachon *J. Solid State Chem*. 133 (1997) 439-444.
13. S.V. Meschel and O.J. Kleppa *Thermochim. Acta* 314 (1998) 205-212.
14. AT. Dinsdale. *Calphad*. 15 (1991) 317–425.
15. F. Sommer, *Z. Metallkde* 73 (1982) 72–86.
16. M. Idbenali ,C. Servant, N. Selhaoui, L. Bouirden, *Calphad* 31 (2007) 479-489.
17. M. Idbenali,C. Servant, N. Selhaoui, L. Bouirden, *Calphad* 33 (2009) 570-575.
18. M. Idbenali,C. Servant, N. Selhaoui, L. Bouirden, *Calphad* 32 (2008) 64-75.
19. Redlich O, Kister A. *IndEng Chem*. 40 (1948) 345-348.
20. B. Jansson, Thesis, Royal Institute of Technology, Stockholm, 1984.
21. S.L. Chen, S. Daniel, Zhang Z, Chang YA, Oates WA, RJ. Schmid Fetzer, *J. Phase Equilib*. 22 (2001) 373-378.

(2018) ; http://www.jmaterenvironsci.com